Chaotic Mixing in a Steady Flow in a Microchannel

Claire Simonnet and Alex Groisman*

Department of Physics, University of California–San Diego, 9500 Gilman Drive, La Jolla, California 92093, USA

(Received 10 December 2004; revised manuscript received 8 February 2005; published 4 April 2005)

We report experiments on mixing of a passively advected fluorescent dye in a low Reynolds number flow in a microscopic channel. The channel is a chain of repeating segments with a custom designed profile that generates a steady three-dimensional flow with stretching and folding, and chaotic mixing. A few statistical characteristics of mixing in the flow are studied and are all found to agree with theoretical and experimental results for the flows in the Batchelor regime of mixing that are chaotic in time. The proposed microchannel provides fast and efficient mixing and is simple to fabricate.

DOI: 10.1103/PhysRevLett.94.134501 PACS numbers: 47.52.+j, 47.60.+i, 83.50.-v, 85.85.+j

The problem of mixing or advection of a passive scalar in turbulent and chaotic flows is one of the fundamental issues in turbulence and chaos [1,2]. It also has practical importance for the dynamics of atmosphere, oceans, and industrial reactors. One of the notable recent advances in the area was a statistical analysis of mixing in the case of a spatially smooth flow, which was first considered by Batchelor [3]. In this Batchelor regime of mixing the strain at all scales originates from the large scale flow and from eddies having dimensions of the whole system. The general theory of mixing in the Batchelor regime, developed in the 1990s [2,4,5], was applicable to smooth chaotic flows with various kinds of time correlations of the velocity field. Later on a practically relevant case of a decay regime was studied, when a field of passive scalar, such as pollutant or dye, is set in the beginning, and no scalar is added in the course of mixing [6]. An additional refinement of the theory took into account effects of solid walls and boundary layers in finite size setups [7,8]. The theory predicted that the mixing length in a chaotic flow in a channel should grow with the Peclet number, Pe, in the flow as $\mathrm{Pe}^{0.25}$ instead of ln(Pe) law expected for an unbounded flow [7,8]. Experimental results on mixing in the chaotic Batchelor regime (CBR) obtained recently in an electromagnetically driven two-dimensional flow [9] and in an elasticity driven three-dimensional (3D) flow of a polymer solution in a channel [10,11] confirmed major predictions of the theory on statistics of passive scalar [9,10] and their dependence on Pe [11].

The chaotic element in mixing in Refs. [9–11] was due to random fluctuations of flow velocity in time. In dynamical systems theory it has long been recognized that mixing can become essentially chaotic in time periodic flows or even steady open flows in channels, if flow lines are diverging exponentially [12–14]. Most recent research on mixing in steady and periodic flows has been in the context of microfluidics [15,16], where a high Reynolds number, Re, which is required for turbulence, is usually impossible to reach. A well documented experimental study of chaotic mixing of dye in a steady flow in a specially patterned microchannel was made by Stroock *et al.* [17]. The authors presented data on spatial distributions of the dye and on the decay of nonhomogeneity of the mixture along the channel. It was not clear, however, whether the decay was exponential as it was found in CBR [6,10,11], and there were no data on probability distribution functions (PDFs) of dye concentration to compare with CBR. Further, the dependence of characteristic mixing length, L_{mix}, on Pe was reported to follow a logarithmic law, $L_{\mathrm{mix}} \sim \ln(\mathrm{Pe})$, instead of $L_{\mathrm{mix}} \sim \mathrm{Pe}^{0.25}$ as found in CBR [7,8,11]. Therefore, regarding similarity of the statistics of chaotic mixing in steady flows and in CBR, the results presented by Stroock *et al.* [17] were either nonconclusive or contradictory.

In this Letter we report experimental results on statistics of mixing of a fluorescent dye in a low Re steady flow in a microscopic channel that agree well with the theoretical [6–8] and experimental [9–11] findings for CBR. The proposed microfluidic mixer is a chain of 34 identical stirring segments with 3D flow, and measurement seg-

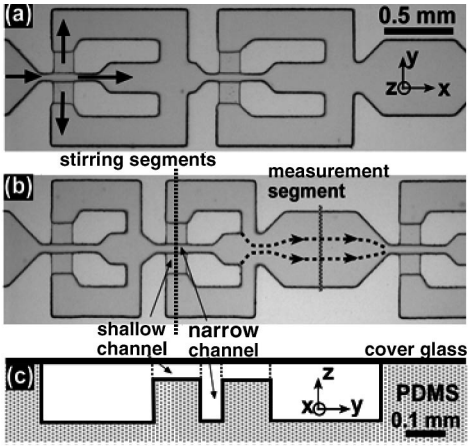

FIG. 1. (a),(b) Micrographs of fragments of the two mixer channels used in the experiments and (c) a schematic drawing of a cross section of a channel. The arrows in (a) show flow directions. The vertical dashed line in (b) indicates the site of the cross section in (c). The hatched area in (b) indicates the region where the confocal microscopy is made. The two dashed lines with arrows in (b) show the lines of merging between the streams from the stirring segment.

ments, where flow is purely longitudinal [Figs. 1(a) and 1(c)]. The design of the stirring segments is somewhat similar to the ''topologic'' mixer introduced recently by Chen and Meiners [18]. The key element generating the 3D flow is a junction between a tall and a narrow main channel (180 μm deep and 50 μm wide) and two shallow (50 μm deep) side channels branching from it at the top. The measurement segments are positioned after every two stirring segments, have a uniform depth of 180 μm, and are 500 μm wide [Fig. 1(a)]. We also studied mixing in a slightly modified version of the channel, Fig. 1(b), with shorter stirring segments of the same profile.

The fabrication protocol for the microfluidic devices shown in Fig. 1 is described in detail elsewhere [17,19]. They were made from a single cast of a silicon elastomer polydimethylsiloxane (PDMS) using the soft lithography. The master mold was fabricated using a two step contact lithography procedure [17,19] and two photomasks with a resolution of 8000 dpi. The master mold had clusters of relief shapes for multiple copies of the microchannels and the resulting molded PDMS devices were identical up to the accuracy of the photomasks and the fidelity of the photolithography.

The working fluid was a 5% solution of Dextran ($M_w \cong 2.5 \times 10^5$ by Polysciences) in a pH = 7.5 phosphate buffer in water, with viscosity, density, and refraction index $\eta = 3.7$ mPa $\cdot$ s [20], $\rho = 1.02$ g/cm^3, and $n = 1.34$, respectively. As the fluorescent passive tracer we used fluorescein-conjugated Dextran (FITC-Dextran) with a molecular mass of 2MDa (supplied by Sigma). It was added to the working liquid at a concentration $c_0 = 240$ ppm. The diffusion coefficient of the FITC-Dextran in water was estimated using the data in Ref. [21] as $D_0 = 7.4 \times 10^{-8}$ cm^2/s. The diffusion coefficient in the working fluid was estimated as $D = 2 \times 10^{-8}$ cm^2/s assuming $D \sim 1/\eta$.

The plain working liquid and the FITC-Dextran solution were fed to the microchannel through two separate inlet ports and the mixture was evacuated from an outlet. The inlets were equally pressurized and the flow was controlled by setting a pressure difference, ΔP, between the inlets and the outlet, which was varied from 32 Pa to 32.5 kPa. The rates of flow from the two inlets were approximately equal, and their ratio was independent of ΔP. The flow driving setup is described in detail elsewhere [19].

To connect ΔP with the flow rate in the channel, we measured the maximal flow velocity in a measurement segment, $\nu_{\max}$, as a function of ΔP using particle tracking. We found $\nu_{\max}$ to increase linearly with ΔP in the whole pressure range, implying a linear flow regime. The relation between the volumetric flow rate, Q, and $\nu_{\max}$ was calculated using Poiseuille flow equations for the measurement segment. We defined Re using the maximal channel depth, $h = 180$ μm, as a length scale and $\bar{\nu} = Q/h^2$ as a representative flow velocity, $\mathrm{Re} = \frac{\bar{\nu} h \rho}{\eta} = \frac{Q\rho}{\eta h}$. In the studied range of ΔP, Re varied from 6.4×10^{-4} to 0.82, which was consistent with the observation of the linear flow regime.

Measurements of spatial distribution of the fluorescent dye were carried out on a confocal microscope (BioRad 1024) using a 20 $\times$, NA = 0.7 WI objective. Stacks of 256 confocal xy scans of 32×1024 pixels each were collected with a step of 0.8 μm in the z direction in the middle of the measurement segments (Fig. 1). Because the flow was purely longitudinal, there were no systematic variations in fluorescence along the x direction. Therefore, the xy scans were averaged to lines of 1024 points (corresponding to 850 μm in the y direction) with a signal to noise ratio of about 8 bits. Finally, 1024×256 points yz-cross section profiles of the channels were assembled out of individual lines and normalized with a profile of a homogeneous FITC-Dextran solution in the channel.

The transformation of the yz profile of dye concentration made by a stirring segment (Fig. 1) can be inferred from the cross sections in Figs. 2(a)–2(c). The flow is split into three streams with significant stretching along the z direction. It is evidenced by a shrinking of the vertical dark strip in the middle about threefold after each step. There is also considerable rotation in the yz plane in the side channels [rounded elements on the sides in Figs. 2(b) and 2(c)]. The three streams merge in the horizontal plane farther downstream that implements folding. The merging lines are two symmetric sharp vertical boundaries [Figs. 2(b)–2(f)] around the central part of the profiles (about 30% of the channel width, corresponding to 40% of the flow).

The result of multiple rotations, stretchings, and foldings is many small scale structures with diffusive smearing at their boundaries [Fig. 2(d)]. To learn more about mixing in the channel we compared yz profiles taken at $N = 6$, where N is the number of segments from the mixer entrance, in three different copies of the same device [Figs. 2(d)–2(f)]. Although the concentration profiles are similar, one can clearly see a variation of the shapes throughout the cross

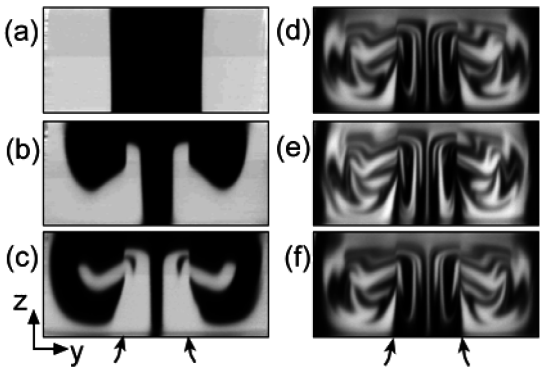

FIG. 2. Confocal micrographs showing distributions of the fluorescent dye over the cross sections of the measurement segments: (a) before the entrance ($N = 0$); (b), (c) and (d)–(f) at $N = 1$, 2, and 6, respectively. Micrographs (d)–(f) correspond to three different copies of the same mixer. The curved arrows at the bottom mark the boundaries between the streams from the stirring segment [cf. Fig. 1(b)].

section. Thus, after multiple applications, the small differences in the transformations by individual stirring segments (due to some variability between the copies) lead to visibly different concentration profiles. This type of behavior is a distinct feature of chaos in the mixing.

Because active 3D flow occurs only in the stirring segments, we defined the characteristic mixing distances in terms of N and NL_s, where L_s is the length of a stirring segment [1.15 and 0.8 mm for the mixers in Figs. 1(a) and 1(b), respectively]. The measurement segments contribute to mixing by increasing the residence time in the flow. Therefore we used a renormalized Peclet number, $\mathrm{Pe} = \frac{\bar{v}h}{D}\frac{2L_s}{2L_s+L_m}$, where $L_m = 0.8$ mm is the length of a measurement segment [Figs. 1(a) and 1(b)]. The mixing was characterized statistically by PDFs of the occurrence of different concentrations, c, of dye over yz profiles. Because of the lower quality of the confocal images near the channel boundaries, statistics were collected only from the inner parts of the cross sections, 0.8×0.8 in depth and width. Plots of PDFs at $\mathrm{Pe} = 2.6 \times 10^5$ and various N are shown in Fig. 3. They represent combined statistics of measurements from three different copies of the mixer in Fig. 1(a). One can see that in the beginning (curve a) the distribution is dominated by two peaks at the original concentrations, 0 and c_0. At advanced stages of mixing (curves d and e) the distributions have a single Gaussian-shaped peak at the average dye concentration, $\bar{c} = c_0/2$ and tails with exponential-like shapes, implying essential intermittency in the mixing. The shapes of the curves d and e are very similar to PDFs found in the experiments on CBR [9,10] and are in good agreement with the theoretical predictions [6].

To evaluate homogeneity of the mixture, we calculated different moments, M_i, of PDFs. An ith moment is defined as an average over a cross section, $M_i \equiv \langle |c - \bar{c}|^i \rangle / \bar{c}^i$. Dependence of the first two moments, M_1 and M_2, on N is shown in Fig. 4(a) for $\mathrm{Pe} = 4 \times 10^3$ and 2.6×10^5. All four dependencies follow exponential decay laws, $M_i \propto \exp(-\gamma_i N)$, with γ_i being greater for M_2 and for smaller Pe. This kind of dependence of M_i on the distance from the entrance was predicted by the theory [7,8] and found in the experiments on CBR [10,11]. We analyzed the dependence of M_i on N at i from 1 to 15 at different Pe and always found exponential decay. Dependence of values of the exponents γ_i on i (data not shown) was linear at small i and an increasing convex function at higher i, in agreement with the experimental findings in CBR [10,11].

We measured the dependence of M_1 and M_2 on N at different Pe (varied by changing ΔP) for the channels in Figs. 1(a) and 1(b) and always found exponential decay, $M_i \propto \exp[-\gamma_i(\mathrm{Pe})N]$. The exponent γ_1 can be used to define a characteristic number of stirring segments required for mixing, $N_{\mathrm{mix}} = 1/\gamma_1$, and mixing length, $L_{\mathrm{mix}} = N_{\mathrm{mix}} L_s$. Dependences of N_{mix} on Pe for the two mixers are shown in Fig. 4(b). They both follow power laws, $N_{\mathrm{mix}} \propto \mathrm{Pe}^{\alpha}$, which are quite distinct from a logarithmic dependence. The exponents α resulting from the power law fits [Fig. 4(b)] were 0.25 ± 0.01 and 0.23 ± 0.02 for the mixers in Figs. 1(a) and 1(b), respectively, in very good agreement with the theoretical prediction [7,8] of $\alpha = 0.25$ and with the recent experimental findings for CBR [11].

As argued by the theory for CBR [7,8], the physical reason for the power law dependence of N_{mix} on Pe is solid boundaries of the channel and boundary layers, where the flow is pure shear and exponential divergence of the flow trajectories is strongly suppressed. The theory also predicts the existence of large fluctuations of c near the boundaries that have been observed experimentally as well [11]. To characterize local fluctuations of c, we introduce a new parameter, $m_2(y) \equiv \langle |c(y) - \bar{c}|^2 \rangle / \bar{c}^2$, where the averaging is made only in the z direction over 40% of the height of the channel near the midplane. The theory suggests that in the regime of exponential decay of M_2, appropriately normalized and time averaged curves $\langle m_2(y)/M_2 \rangle$ should be in-

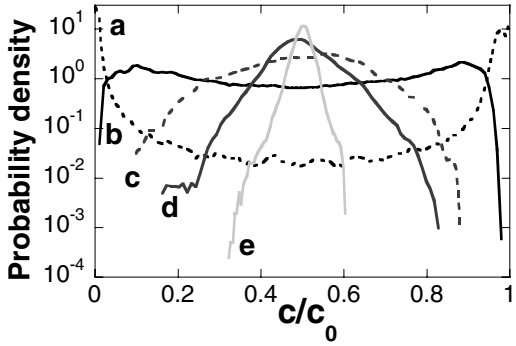

FIG. 3. Plots of PDF of the concentration of the fluorescent dye at $\mathrm{Pe} = 2.6 \times 10^5$ and different positions. Curves a, b, c, d, and e correspond to $N = 0$, 4, 10, 14, and 22, respectively.

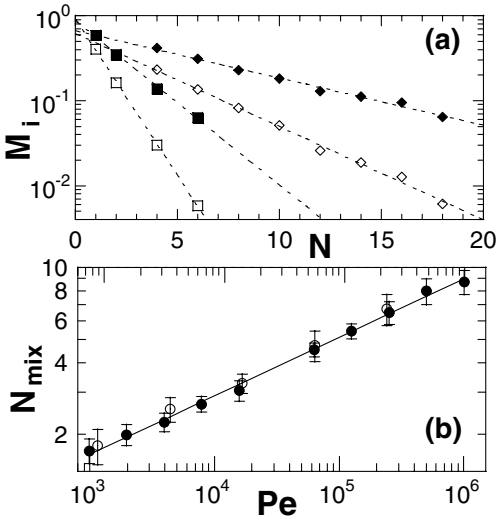

FIG. 4. (a) The moments M_1 (solid symbols) and M_2 (open symbols) of PDF of the dye concentration as functions of N at $\mathrm{Pe} = 4.0 \times 10^3$ (squares) and $\mathrm{Pe} = 2.6 \times 10^5$ (diamonds). (b) The mixing length, N_{mix}, as a function of Pe for the mixers in Figs. 1(a) and 1(b), solid and open symbols, respectively. The solid line is a power law fit.

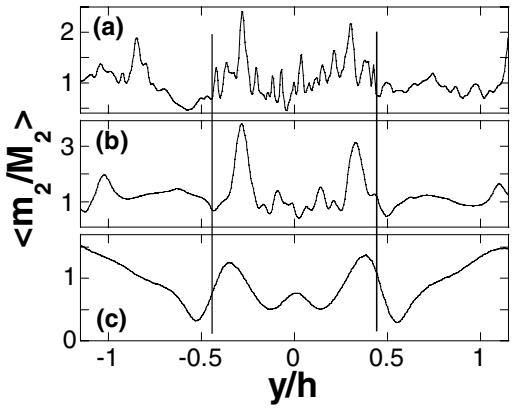

FIG. 5. Spatial dependence of $\langle m_2(y)/M_2\rangle$ on the position, y, across the microchannel measured from the center: (a) Pe $= 1.0 \times 10^6$, (b) Pe $= 2.6 \times 10^5$, and (c) Pe $= 1.0 \times 10^3$. The vertical lines show the locations of the boundaries between the three merging streams [cf. Figs. 1(b) and 2].

dependent of M_2. Therefore we calculated $\langle m_2(y)/M_2\rangle$ for eight different values of Pe from 10^3 to 10^6 with averaging over various N and various copies of the mixer. Three representative plots of $\langle m_2(y)/M_2\rangle$ (at Pe $= 10^3$, 2.6×10^5 and 10^6) are shown in Fig. 5.

The common feature of the curves in Fig. 5(c) is two symmetric peaks near the boundaries (dashed lines), which separate the three streams coming from a stirring segment [see Figs. 1(b) and 2]. Positions of the peaks correspond to the boundary layers near the side walls in the upstream narrow main channels [Fig. 1(b)] that are advected to the measurement segments. Therefore the peaks can be considered evidence of large fluctuations of c in the boundary layers. From examining the shape of the stirring segment in Fig. 1 and concentration profiles in Figs. 2(a)–2(c) it is plausible to argue that the liquid in those boundary layers is subjected to almost pure shear flow. Although the peaks appear to shift away from the boundaries (dashed lines in Fig. 5) with increasing Pe (that is not observed in CBR), their location is in general agreement with the theory [7,8] and experiments on CBR [11]. The width of the peaks becomes smaller at higher Pe, which also agrees with the CBR theory and experiments.

Summarizing the experimental results on statistics of mixing in the microchannel (Figs. 3–5) we note that they are in good agreement with the theoretical predictions for CBR [6–8]. Further, the exponential decay of M_i with distance from the mixer entrance [Fig. 4(a)] is fully consistent with the experimental findings in CBR [10,11], and PDFs of dye distribution (Fig. 3) have a close similarity to those found in CBR [9,10]. Therefore, although the flow in the microchannel is steady and is chaotic only in the sense of divergence of flow lines [12–14], the mixing has essentially the same statistics as in CBR, where flow is chaotic in time.

The proposed mixer also turns out to be a convenient system to study the dependence of various parameters on Pe. So, the relation $L_{\mathrm{mix}} \propto \mathrm{Pe}^{0.25}$ is established over 3 orders of magnitude in Pe, compared with a 1.5 order of magnitude range in Ref. [11]. Finally, the mixer in Fig. 1(b) has a high practical efficiency. Its characteristic mixing length is more than twice shorter than in Ref. [17], when measured in units of channel depths, h, at the same Pe. The proposed mixer is also advantageous compared to the device in Ref. [18] (which may have the same or higher efficiency), because it is made out of a single cast of PDMS and does not require assembly.

We are grateful to M. Chertkov and V. Lebedev for multiple illuminating discussions and theoretical guidance. We thank D. Kleinfeld for allowing us to use his time share on the confocal microscope. The work was partially funded by Binational U.S.–Israel foundation Grant No. 2002235.

*To whom all correspondence should be addressed.
Electronic address: agroisman@ucsd.edu

[1] Z. Warhaft, Annu. Rev. Fluid Mech. **32**, 203 (2000).
[2] G. Falkovich, K. Gawedzki, and M. Vergassola, Rev. Mod. Phys. **73**, 913 (2001).
[3] G. K. Batchelor, J. Fluid Mech. **5**, 113 (1959).
[4] B. I. Shraiman and E. D. Siggia, Phys. Rev. E **49**, 2912 (1994).
[5] M. Chertkov, G. Falkovich, I. Kolokolov, and V. Lebedev, Phys. Rev. E **51**, 5609 (1995).
[6] E. Balkovsky and A. Fouxon, Phys. Rev. E **60**, 4164 (1999).
[7] M. Chertkov and V. Lebedev, Phys. Rev. Lett. **90**, 034501 (2003).
[8] V. V. Lebedev and K. S. Turitsyn, Phys. Rev. E **69**, 036301 (2004).
[9] M.-C. Jullien, P. Castiglione, and P. Tabeling, Phys. Rev. Lett. **85**, 3636 (2000).
[10] A. Groisman and V. Steinberg, Nature (London) **410**, 905 (2001).
[11] T. Burghelea, E. Segre, and V. Steinberg, Phys. Rev. Lett. **92**, 164501 (2004).
[12] H. Aref, J. Fluid Mech. **143**, 1 (1984).
[13] T. H. Solomon and I. Mezic, Nature (London) **425**, 376 (2003).
[14] S. Wiggins and J. M. Ottino, Philos. Trans. R. Soc. London A **362**, 937 (2004).
[15] R. H. Liu, M. A. Stremler, K. V. Sharp, M. G. Olsen, J. G. Santiago, R. J. Adrian, H. Aref, and D. J. Beebe, J. Microelectromech. Syst. **9**, 190 (2000).
[16] J. M. Ottino and S. Wiggins, Philos. Trans. R. Soc. London A **362**, 923 (2004).
[17] A. D. Stroock, S. K. Dertinger, A. Ajdari, I. Mezic, H. Stone, and G. M. Whitesides, Science **295**, 647 (2002).
[18] H. Chen and J.-C. Meiners, Appl. Phys. Lett. **84**, 2193 (2004).
[19] A. Groisman, M. Enzelberger, and S. R. Quake, Science **300**, 955 (2003).
[20] W. Akers and M. A. Haidekker, J. Biomech. Eng. **126**, 340 (2004).
[21] C. Wu, Macromolecules **26**, 3821 (1993).